Transcranial Ultrasound Focus Reconstruction with Phase and Amplitude Correction

Jason White, Greg T. Clement, and Kullervo Hynynen, *Member, IEEE*

Abstract*—Therapeutic and diagnostic ultrasound procedures performed noninvasively through the skull require a reliable method for maintaining acoustic focus integrity after transmission through layered bone structures. This study used a multiple-element, phased-array transducer to reconstruct ultrasound foci through the human skull by amplitude and phase correction. It was previously demonstrated that adaptive phase correction using a multiple-element, focused transducer array yields a significant correction to an acoustic field that has been distorted by the heterogeneities of the skull bone. The introduction of amplitude correction, in a regime in which acoustic pressures from individual transducer array elements are adjusted to be normalized at the focus, has demonstrated a 6% (−0.27 dB) average decrease in acoustic sidelobe acoustic intensity relative to the focal intensity and a 2% (−0.09 dB) average decrease in the full-width-at-half-maximum (FWHM) of the acoustic intensity profile at the focus. These improvements come at the expense of significant ultrasound intensity loss—as much as 30% lower (−1.55 dB)—at the focus because the amplitude correction method requires that, at constant power, a larger proportion of energy is absorbed or reflected by regions of the skull that transmit less energy. In contrast, a second correction method that distributes pressure amplitudes such that the sections of the skull which transmit more ultrasound energy are exposed with higher ultrasound intensities has demonstrated an average sidelobe intensity decrease of 3% (−0.13 dB) with no change in the FWHM at the focus. On average, there was a 2% (0.09 dB) increase in the acoustic intensity at the focus for this inverse amplitude correction method. These results indicate that amplitude correction according to the transmission properties of various segments of the skull have a clear effect on ultrasound energy throughput into a target site within the brain parenchyma.

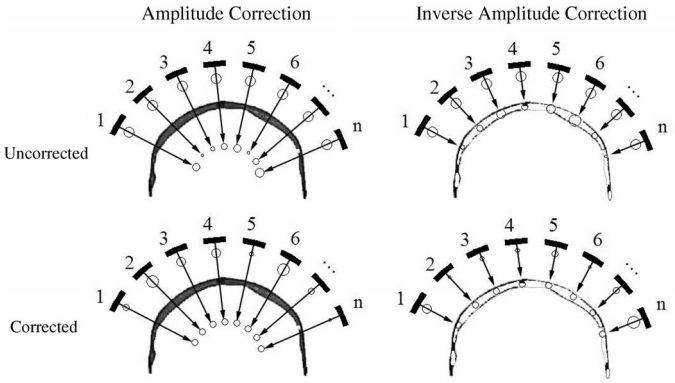

Fig. 1. A schematic representation of the two amplitude correction methods. A sectioned transducer is driven at powers proportional to the size of the circles adjacent to the transducer elements. The upper-left diagram demonstrates the variable pressure levels at the focus for each transducer element after transmission through the skull. The lower-left diagram indicates how a corrected amplitude distribution would normalize the pressures from each element at the focus. The upper-right diagram indicates the variable energy absorption for each region of the skull. The lower-right diagram indicates the results of an amplitude correction that would inversely compensate for absorption in the skull bone.

I. Introduction

The focusing of ultrasound through the human skull has been investigated for several therapeutic and diagnostic applications [1], such as the treatment of brain tumors [2]–[4], targeted drug delivery [5], thrombolytic stroke treatment [6], blood flow imaging [7], [8], detecting internal bleeding [9], and tomographic brain imaging [10]–[14]. The ultrasonic attenuating and distorting characteristics of skull bone has been a limiting factor for the successful implementation of this technique. The development of large-area, multiple-element transducer arrays has demonstrated the potential for the correction of distorted acoustic fields within the cranial cavity [15]. The reconstruction of an acoustic focus within the brain with these arrays has been demonstrated by adjusting the individual phases of each transducer array element to reestablish phase coherence after transmission through the skull. To further examine the possibility of optimizing focal reconstruction through the skull, amplitude correction filters are implemented based on suggestions [16]–[18] that a compensation for the attenuating effects of bone that recreates a uniform acoustic wavefront will reduce acoustic sidelobe structures and refine the quality of the focus.

This study examines the effects of an amplitude correction scheme that renormalizes a spherical wavefront after transmission through spatially inhomogeneous media, such as the human skull, that distorts the acoustic intensity field. The objective, schematically shown in Fig. 1, is to determine if the normalization of pressure amplitudes from each source at the focus of a 448-element spherical transducer array can improve the reconstructed beam pattern after transmission through the absorbing layers of ex vivo human skull. The reduction of diffraction sidelobes and the restoration of focal integrity will improve the diagnostic and therapeutic effectiveness of a transcranial ultrasound system.

Manuscript received November 17, 2004; accepted February 4, 2005. This work was supported by grant R01 EB003268 from the National Institutes of Health.

The authors are with the Department of Radiology, Harvard Medical School, Brigham and Women's Hospital, Boston MA 02115 (e-mail: white@bwh.harvard.edu).

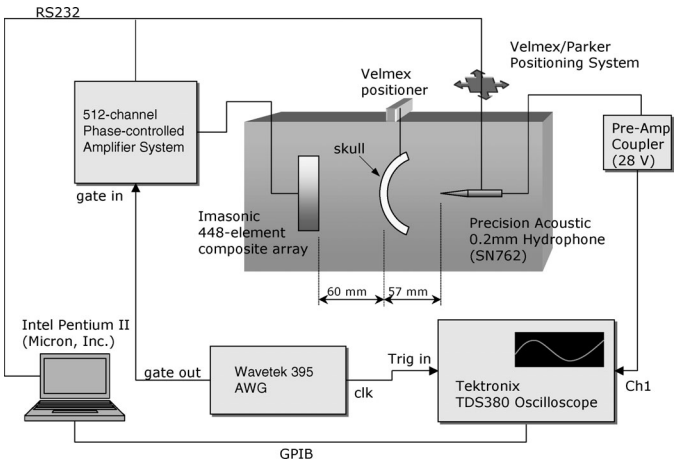

Fig. 2. Experimental setup.

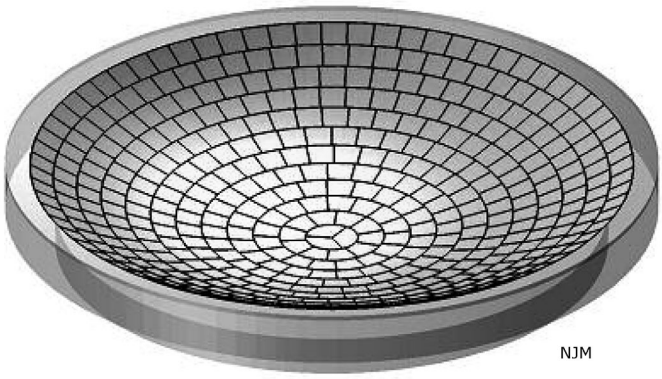

Fig. 3. A 448-element, spherically focused 1-3 composite array with a 120 mm radius of curvature and an active diameter of 120 mm.

In addition, the opposite amplitude correction modality that distributes acoustic pressure amplitudes with preference to those sections of the skull that transmit more energy is explored. This inverse correction is schematically described in Fig. 1. Although this amplitude filter exaggerates the distortions of the wavefront arriving at the focus, it will improve the efficiency of power transmission and reduce localized skull heating that has been shown to result from the transmission of ultrasound in transcranial applications [19].

II. Methods

Four ex vivo human calvaria fixed in 10% buffered formaldehyde were submerged in degassed (between 1 and 2 ppm dissolved oxygen content), deionized water for the experiments. The acoustic properties of fixed human calvaria were assumed to be similar to those of fresh specimens [20]. Each calvarium was mounted by six brass setscrews onto an acrylic frame, which then was positioned between the sonicating transducer and the receiving hydrophone as shown in Fig. 2. The skull mount allowed for variable positioning normal to the sonicating transducer's axis of propagation at a resolution of 0.5 mm so that multiple points on the skull could be sonicated. As illustrated in Fig. 3, a 448-element, 1-3 composite spherically focused array with a diameter of 120 mm and a radius-of-curvature of 120 mm (Imasonic, Lyon, France) was operated at 1.1 MHz. No lens was placed between the transducer and the skull for focus elevation. A 0.2 mm diameter polyvinylidene fluoride (PVDF) needle hydrophone (Precision Acoustics, Dorchester, England) was used as the ultrasound receiver. The receiver directivity response for the operating frequency was measured to be -3 dB at 80° away from the principal axis; therefore, the directivity was negligible for the range of incident angles in this study. It was positioned at the geometric focus of the transducer array and spatially scanned by a stepping-motor-controlled three-dimensional (3-D) positioning system (Parker, Hannifin, PA). The receiver response was recorded by a personal computer (Toshiba, Tokyo, Japan) interfaced by an IEEE 488 data bus to a digital oscilloscope (Tektronics Model 380, Beaverton, OR). The computer also served as the position controller for the scanning hydrophone. In this study, the acoustic fields both before and after insertion of the skull were recorded for a 10 mm^2 area of the plane normal to the acoustic propagation axis at a scanning resolution of 0.2 mm.

The 448-element array was driven by a 256-channel phase-and-amplitude controllable amplifier system [21] in pulse-mode (PRF = 200 Hz, 60λ, duty cycle = 1.1%) to eliminate standing wave patterns set up by the experimental tank. To avoid additional interactions with reflected waves, the tank was lined with anechoic rubber, and the hydrophone mount was encased in silicone rubber. The array was driven in two separate stages (channels 1–256 then channels 257–448) for each field measurement; the resulting scans were superimposed numerically to create the composite scan [15].

Each calvarium was placed approximately 60 mm from the face of the transducer and moved in increments of 8.0 mm perpendicular to the axis of propagation for three successive sampling points, for a total of 12 data points. Shifting the skulls laterally gave a negligible change in the transducer-skull distance (<1 mm) and was not included as a parameter in the analysis. At each point, the hydrophone phase and amplitude response at the focus was recorded for each of the 448 elements. This data, in combination with the same data produced with no skull specimen in place, gave the phase and amplitude distortion information that then was used for correction. Phase correction factors were created by phase matching all channels to the first channel's received waveform [22] according to:

$$\Delta\phi(r_b) = \arg\left(\frac{P(r_a)}{P_0(r_a)}P_0(r_b)\right). \tag{1}$$

Amplitude correction to normalize wavefront amplitudes was accomplished by proportionally reducing all channels relative to the channel with the lowest pressure

transmission value, which was set at the highest transmission ratio. The corrected amplitude coefficients are:

$$A_c = \frac{A_{\min}}{A_0}, \tag{2}$$

where A_c is the corrected amplitude coefficient, $A_{\min}$ is the amplitude of the channel with the lowest transmission value, and A_0 is the uncorrected amplitude coefficient.

The inverse correction was accomplished by proportionally increasing the output of the array elements that yield a higher acoustic transmission through the skull. The coefficients for the inverse amplitude correction are given by:

$$A_c = \frac{A_0}{A_{\max}}, \tag{3}$$

where A_c is the corrected amplitude coefficient, $A_{\max}$ is the amplitude of the channel with the highest transmission value, and A_0 is the uncorrected amplitude coefficient.

For each point on each of the calvarium specimens, a scan was performed for sonications with phase-and-amplitude correction (both amplitude correction methods), phase correction only, and no correction. In these experiments, the total radio frequency (RF) power delivered to the transducer by the driving system was kept constant at 10 W for each sonication.

III. Results

Without applying phase or amplitude correction to the driving signals, a 1.1 MHz gated ultrasound signal was transmitted through each of the four ex vivo calvarium specimens at each of the three spatial settings for a total of 12 sample points. The planar scans normal to the propagation axis of the transducer revealed a highly distorted acoustic field in which the original focus was observed to be shifted spatially (on average 1.5 mm) and often split into multiple foci. When phase correction was implemented, a single focus of significantly increased acoustic intensity—a factor of 11.5 increase at the focus on average—was reconstructed at the intended focal point. When amplitude correction was included in the correction, all instances showed a decrease in acoustic intensity at the focus. Results while maintaining a constant output acoustic power, as shown in Fig. 4, indicate a 17% (−0.81 dB) average decrease of the acoustic intensity at the focus after the inclusion of amplitude correction. The maximum observed decrease in intensity was 30% (−1.55 dB). It also was observed that, after amplitude correction, the sidelobe structures in relation to the acoustic intensity at the focus was suppressed in 8 out of 10 instances, for an average relative decrease of 6% (−0.27 dB) and an observed maximum decrease of 13% (−0.60 dB)—2 samples out of the 12 were discarded because no sidelobe structures could be clearly identified. The full-width-at-half-maximum (FWHM) of the focus intensity also was observed in 8 out of the 12 cases to decrease proportionally with amplitude correction for an average reduction of 2% (−0.09 dB). These results are all shown in Fig. 4.

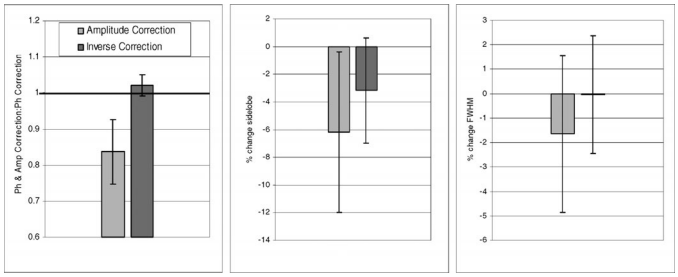

Fig. 4. The left graph compares the relative intensity change at the focus for the two amplitude correction methods. The center graph compares the sidelobe intensity changes as a percentage of the focal intensity for the two amplitude correction methods. The right graph compares the change in FWHM of the focal intensity profiles for the two amplitude correction methods. The total power delivered for each sonication was 10 W.

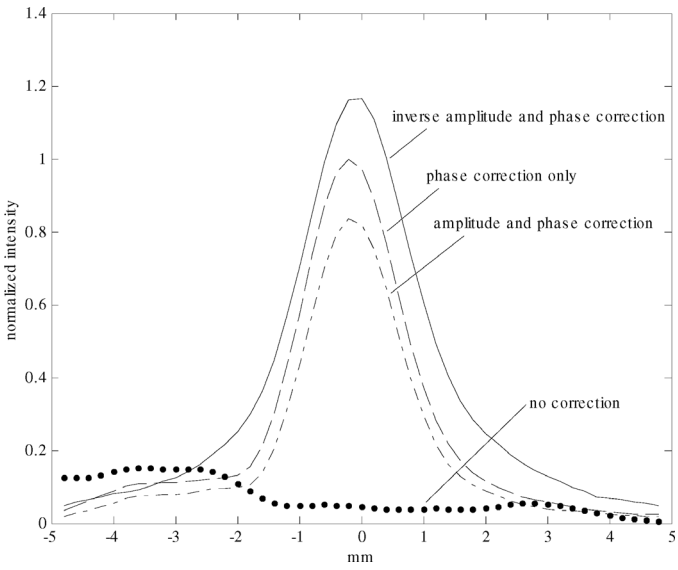

Fig. 5. Relative acoustic intensity profile across the focal plane of a sample sonication for the four cases of no correction, phase correction only, amplitude correction (with phase correction), and inverse amplitude correction (with phase correction). The plots have been normalized to the phase-correction-only intensity profile.

The combination of phase correction with inverse amplitude correction yielded a focal intensity decrease in five of the experimental samples and an increase for the remaining seven samples for an overall average intensity increase of 2% (0.09 dB). It was observed that, after inverse amplitude correction, the sidelobe structures in relation with the intensity at the focus was suppressed in 9 out of 10 instances for an average decrease of 3% (−0.13 dB). No change was observed for the FWHM of the focus intensity. These results are shown in conjunction with the results from the former correction method in Fig. 5.

Figs. 5 and 6 are contour plots and cross-sectional plots, respectively, for one sample of the acoustic intensity field measured from the four sonication scenarios of no correction, phase correction only, amplitude correction (with phase correction), and inverse amplitude correction (with phase correction). The cross-sectional plots of Fig. 5 were

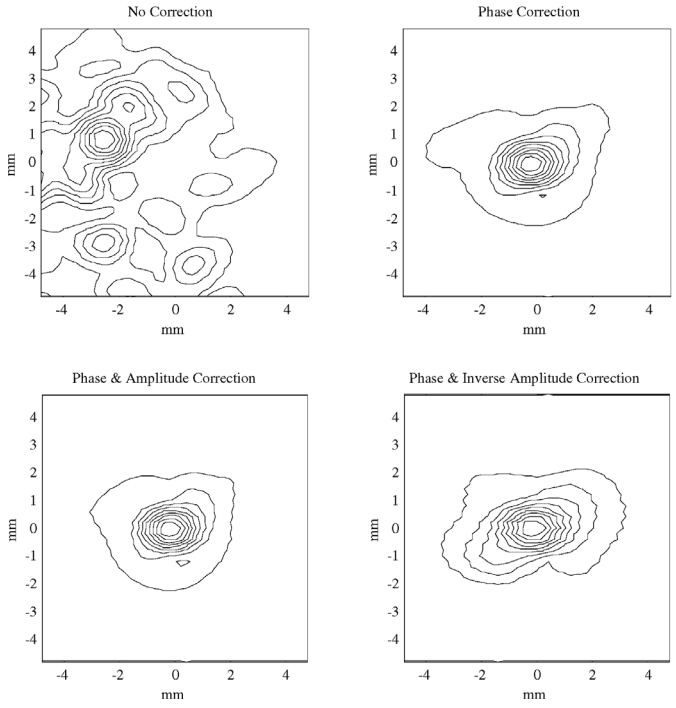

Fig. 6. Contour plots (10% contours) of the acoustic intensity measured at the focus for the four cases of no correction, phase correction only, amplitude correction (with phase correction), and inverse amplitude correction (also with phase correction). The total power delivered for each sonication was 10 W. Cross-sectional intensity profiles for each of these contour plots are presented in Fig. 5.

obtained by selecting and plotting the horizontal vector through the centers of the contour plots of Fig. 6.

IV. Discussion

The objective of this study was to examine and evaluate an amplitude correction method that homogenizes the acoustic intensity across a wavefront to improve ultrasound focal reconstruction after transmission through the human skull. The combination of established, multiple-element phase correction techniques [22] with amplitude correction should yield an observable decrease in acoustic sidelobe magnitude and an improvement in focus quality. However, due to the nature of the amplitude correction method, the focal intensity was reduced by 17% (−0.81 dB) on average because a larger portion of the total power was diverted to segments of the skull that transmit less energy. For applications in which high power is required, this correction method potentially could lead to excessive localized bone heating.

The opposite correction method that inversely biases the amplitudes such that skull segments which transmit less energy were exposed to proportionally lower ultrasound energies was hypothesized to yield the opposite effect so that a higher focal intensity, a relative increase in sidelobe magnitude, and an increase FWHM should be observed after this correction. In contrast to the hypothesis, relative sidelobe intensity and the FWHM of the focal profile remained statistically unchanged after application of the inverse amplitude correction method. The most significant observable difference in the two correction methods was the nearly unchanged focal acoustic intensity in the inverse amplitude correction method—2% (0.09 dB) average increase—as compared to the consistently reproducible and appreciable drop in focal energy—17% (−0.81 dB) average decrease—when the former amplitude correction method was implemented. Changes in sidelobe levels and FWHM for both corrections are minor as compared to changes at the focus.

V. Conclusions

For high-power applications, the observation of a reduction in focal ultrasound intensity indicates a serious disadvantage to the application of a wavefront amplitude correction that redirects energy to less transmitting areas of the skull. Minor improvements in the sidelobe magnitude and focal FWHM may not be sufficient to justify the decreased level of energy delivery at the focus. However, an inverse amplitude correction maintained the acoustic intensity at the focus and did not significantly alter the sidelobes or the beam profile. Because of this, the inverse amplitude correction is a more likely candidate for the investigation of amplitude correction effects in transcranial ultrasound applications.

References

[1] G. T. Clement and K. Hynynen, "Correlation of ultrasound phase with physical skull properties," *Ultrasound Med. Biol.*, vol. 28, pp. 617–624, Feb. 2002.

[2] F. J. Fry, "Transkull transmission of an intense focused ultrasonic beam," *Ultrasound Med. Biol.*, vol. 3, no. 2–3, pp. 179–184, 1977.

[3] J. Tobias, K. Hynynen, R. Roemer, A. N. Guthkelch, A. S. Fleischer, and J. Shively, "An ultrasound window to perform scanned, focused ultrasound hyperthermia treatments of brain tumors," *Med. Phys.*, vol. 14, pp. 228–234, Mar. 1987.

[4] M. Tanter, J. L. Thomas, and M. Fink, "Focusing and steering through absorbing and aberrating layers: Application to ultrasonic propagation through the skull," *J. Acoust. Soc. Amer.*, vol. 103, pt. 1, pp. 2403–2410, May 1998.

[5] J. R. Tacker and R. U. Anderson, "Delivery of antitumor drug to bladder cancer by use of phase transition liposomes and hyperthermia," *J. Urol.*, vol. 127, pp. 1211–1214, June 1982.

[6] S. Behrens, K. Spengos, M. Daffertshofer, H. Schroeck, C. E. Dempfle, and M. Hennerici, "Transcranial-ultrasound-improved thrombolysis: Diagnostic vs. therapeutic ultrasound," *Ultrasound Med. Biol.*, vol. 27, pp. 1683–1689, 2001.

[7] F. J. Kirkham, T. S. Padayachee, S. Parsons, L. S. Seargeant, and F. R. House, "Transcranial measurement of blood flow velocities in the basal cerebral arteries using pulsed Doppler ultrasound," *Ultrasound Med. Biol.*, vol. 12, pp. 15–21, 1986.

[8] T. Postert, P. Hoppe, J. Federlein, H. Przuntek, T. Buttner, S. Helbeck, H. Ermert, and W. Wilkening, "Ultrasonic assessment of brain perfusion," *Stroke*, vol. 31, pp. 1460–1462, June 2000.

[9] M. A. Moehring, B. P. Wilson, and K. W. Beach, "Intracranial bleed monitor," in *Proc. IEEE Ultrason. Symp.*, 1999, pp. 1545–1549.

[10] F. J. Fry, R. C. Eggleton, and R. F. Heimburger, "Transkull visualization of brain using ultrasound; An experimental model study," *Exerpta Medica*, pp. 97–103, 1974.

[11] P. L. Carson, T. V. Oughton, W. R. Hendee, and A. S. Ahuja, "Imaging soft tissue through bone with ultrasound transmission tomography by reconstruction," *Med. Phys.*, vol. 4, pp. 302–309, July 1977.

[12] S. W. Smith, D. J. Phillips, O. T. von Ramm, and F. L. Thurstone, "Some advances in acoustic imaging through the skull," *Nat. Bur. Standards Pub. #525*, pp. 209–218, 1979.

[13] K. A. Dines, F. J. Fry, J. T. Patrick, and R. L. Gilmor, "Computerized ultrasound tomography of the human head: Experimental results," *Ultrason. Imag.*, vol. 3, pp. 342–351, Oct. 1981.

[14] J. Ylitalo, J. Koivukangas, and J. Oksman, "Ultrasonic reflection mode computed tomography through a skull bone," *IEEE Trans. Biomed. Eng.*, vol. 37, pp. 1059–1066, Nov. 1990.

[15] G. T. Clement, J. White, and K. Hynynen, "Investigation of a large-area phased array for focused ultrasound surgery through the skull," *Phys. Med. Biol.*, vol. 45, pp. 1071–1083, Apr. 2000.

[16] J. Thomas and M. A. Fink, "Ultrasonic beam focusing through tissue inhomogeneities with a time reversal mirror: Application to transskull therapy," *IEEE Trans. Ultrason., Ferroelect., Freq. Contr.*, vol. 43, no. 6, pp. 1122–1129, 1996.

[17] J. F. Aubry, M. Tanter, M. Pernot, J. L. Thomas, and M. Fink, "Experimental demonstration of noninvasive transskull adaptive focusing based on prior computed tomography scans," *J. Acoust. Soc. Amer.*, vol. 113, pp. 84–93, Jan. 2003.

[18] M. Tanter, J. L. Thomas, and M. Fink, "Time reversal and inverse filter," *J. Acoust. Soc. Amer.*, vol. 108, pp. 223–234, July 2000.

[19] E. L. Carstensen, S. Z. Child, S. Norton, and W. Nyborg, "Ultrasonic heating of the skull," *J. Acoust. Soc. Amer.*, vol. 87, pp. 1310–1317, Mar. 1990.

[20] F. J. Fry and J. E. Barger, "Acoustical properties of the human skull," *J. Acoust. Soc. Amer.*, vol. 63, pp. 1576–1590, May 1978.

[21] D. R. Daum, M. T. Buchanan, T. Fjield, and K. Hynynen, "Design and evaluation of a feedback based phased array system for ultrasound surgery," *IEEE Trans. Ultrason., Ferroelect., Freq. Contr.*, vol. 45, no. 2, pp. 431–438, 1998.

[22] G. T. Clement and K. Hynynen, "Micro-receiver guided transcranial beam steering," *IEEE Trans. Ultrason., Ferroelect., Freq. Contr.*, vol. 49, no. 4, pp. 447–453, 2002.